DOI 10.1007/s10778-020-01031-9
International Applied Mechanics, Vol. 56, No. 4, July, 2020

THREE-DIMENSIONAL ANALYSIS OF THE FREE VIBRATIONS OF LAYERED COMPOSITE PLATES BASED ON THE SEMIANALYTIC FINITE-ELEMENT METHOD

A. V. Marchuk, S. V. Reneiskaya, and O. N. Leshchuk

The spatial theory of elasticity is used to develop two variants of the semianalytic finite-element method for studying the frequencies of free vibrations and modes of distribution of displacements in them. The calculation by the two methods serves as a proof of the reliability of the analysis. The frequencies of free vibrations and the corresponding modes of distribution of displacements in a layered composite plate with two opposite boundaries free and the other two hinged are analyzed. A plate with a free lower surface, which is clamped to the lower surface and leaning on an elastic layer with finite thickness and inertial properties is considered. The high accuracy of the proposed models in these problems is demonstrated. It is pointed out that the inertial properties of the foundation should not be neglected.

Keywords: 3D analysis, semianalytical finite-element method, sandwich composite panel, free vibrations

Introduction. The use of structural composite systems, in particular layered ones that are substantially orthotropic and have constituent materials with essentially different moduli of elasticity has been increasing. They are in complicated deformation conditions, have different boundary and interface conditions, and are subject to dynamic loads close to resonance. These features can lead to three-dimensional dynamic deformation.

The use of direct exact methods of the spatial theory of elasticity for studying the free vibrations of such structures is significantly complicated and limited to the consideration of hinged plates. In particular, such problems were considered in [2, 26, 29]. Classical approaches based on simplified Kirchhoff–Love hypotheses can lead in certain cases to significant errors in the characteristics of free vibrations. Therefore, various refined versions of theories for studying the dynamic behavior of layered structures continue to be developed [2, 11–14, 17, 20, 33, 36–38, etc.]. Different refined models were used in [2, 4–10, 18, 19, 22, 23, 25, 33–37, 39–42, etc.] to study dynamic deformation. Various numerical-analytical methods of three-dimensional analysis of layered structures continue to be developed [1, 3, 9, 11, 12, 15, 16, 21, 24, 30–32, 43]. Despite the abundance of studies on the dynamic deformation of layered plates, we failed to find three-dimensional analyzes of the free vibrations of plates with two opposite boundaries free and the other two hinged on an elastic layer with finite thickness and inertial properties, and also on a perfectly rigid foundation. Such a case can be an integral part of a design model of transport facilities.

Problem Statement. The goal of this paper is to develop two versions of the semianalytical finite-element method that allow analyzing the free vibrations of layered composite plates. In the first version of the semianalytical finite-element method, to approximate the desired functions in the planar X coordinate, a finite-element approximation is used. The unknown functions in the Y coordinate are represented as Fourier series, and the known polynomials are used in thickness (Z coordinate) [29]. In the second version, polynomials are used to approximate the unknown functions in the plan in the X coordinate, Fourier series is used in the Y coordinate, and the distribution of the unknown functions over the thickness of the structure is found based on the analytical solution of the corresponding system of differential equations [28]. Solving problems by two methods in to find the

National Transport University, 1 Mykhaila Omelyanovycha-Pavlenka St. Kyiv, Ukraine 01010; email: sm_ntu@ukr.net. Translated from Prikladnaya Mekhanika, Vol. 56, No. 4, pp. 97–116, July–August 2020. Original article submitted February 12, 2019.

frequencies of free vibrations and modes of distribution of displacements in them serves as an additional validation of the calculated results. They do not compete but supplement each other. When determining the frequencies of free vibrations in a model with an analytical solution of the corresponding system of differential equations for the unknown functions over the thickness of the plate, the frequencies obtained from the model with a polynomial approximation of the unknown functions over the thickness are used as starting points.

Using Fourier series for the approximation in plan in the Y coordinate in both versions introduces well-known restrictions on the boundary conditions. A finite element approximation is used along the X coordinate, which significantly expands the range of boundary conditions that can be considered (hinged, free, clamped). It is possible to consider perfect bonding of the layers or sliding of the layers along a part of the surface perpendicular to the X coordinate. The combination of conditions at the interface between the layers and on the boundary allows the consideration of composite structures with complex configuration throughout the thickness perpendicular to the X coordinate. Due to the limited scope of the article, we restrict ourselves to the consideration of the free vibrations of plates with a hinged edge along the X coordinate (a common case in design models of transport structures). Structures with a free lower surface, with forbidden displacements on the lower surface and resting on a foundation modeled by a layer of finite thickness and having inertial properties are considered.

Consider a layered structure with composite layers with three planes of elastic symmetry (orthotropic layers). The physical and mechanical characteristics of orthotropic layers are related by

$$e_{11}^{(k)}=\frac{\sigma_{11}^{(k)}}{E_1^{(k)}}+\frac{\nu_{21}^{(k)}\sigma_{22}^{(k)}}{E_2^{(k)}}+\frac{\nu_{31}^{(k)}\sigma_{33}^{(k)}}{E_3^{(k)}},\qquad e_{22}^{(k)}=\frac{\nu_{12}^{(k)}\sigma_{11}^{(k)}}{E_1^{(k)}}+\frac{\sigma_{22}^{(k)}}{E_2^{(k)}}+\frac{\nu_{32}^{(k)}\sigma_{33}^{(k)}}{E_3^{(k)}},$$

$$e_{33}^{(k)}=\frac{\nu_{13}^{(k)}\sigma_{11}^{(k)}}{E_1^{(k)}}+\frac{\nu_{23}^{(k)}\sigma_{22}^{(k)}}{E_2^{(k)}}+\frac{\sigma_{33}^{(k)}}{E_3^{(k)}},\qquad 2e_{23}^{(k)}=\frac{\sigma_{23}^{(k)}}{G_{23}^{(k)}},\qquad 2e_{13}^{(k)}=\frac{\sigma_{13}^{(k)}}{G_{13}^{(k)}},\qquad 2e_{12}^{(k)}=\frac{\sigma_{12}^{(k)}}{G_{12}^{(k)}}.$$

The superscript (k) indicates a layer number. Directions 1, 2, and 3 are identical to the directions X, Y, Z, respectively. The Z-axis is directed downward. In the second section, the summation is over the subscripts l and p ($l=1,2,3$, $p=1,2,3$).

1. Version of the Semianalytical Finite-Element Method for Studying the Free Vibrations Based on a Polynomial Approximation overe the Thickness of the Structure (V1).

We represent the vector of the required displacements as follows:

$$U_1^{(k)}(x,y,z,t)=U_{1l}^{(k)}(x,y,t)f_{1l}^{(k)}(z),$$

$$U_2^{(k)}(x,y,z,t)=U_{2l}^{(k)}(x,y,t)f_{2l}^{(k)}(z),$$

$$U_3^{(k)}(x,y,z,t)=W_p^{(k)}(x,y,t)\beta_p^{(k)}(z). \tag{1.1}$$

Here $U_{11}^{(k)}(x,y,t)$ are the tangential displacements on the upper surfaces of the kth layer along the X-axis; $U_{12}^{(k)}(x,y,t)$ are the tangential displacements on the lower surface of the kth layer along the X-axis; $U_{13}^{(k)}(x,y,t)$ are the shear functions along the X-axis; $U_{21}^{(k)}(x,y,t)$, $U_{22}^{(k)}(x,y,t)$, $U_{23}^{(k)}(x,y,t)$ are the tangential displacements on the faces of the kth layer and the shear function along the Y-axis; $W_1^{(k)}(x,y,t)$, $W_2^{(k)}(x,y,t)$ are the normal displacements on the faces of the kth layer; $W_3^{(k)}(x,y,t)$ is the compression function; $f_{11}^{(k)}(z)$, $f_{12}^{(k)}(z)$, $f_{21}^{(k)}(z)$, $f_{22}^{(k)}(z)$, $\beta_1^{(k)}(z)$, $\beta_2^{(k)}(z)$ are given polynomials of the first degree; $\beta_3^{(k)}(z)$ is a polynomial of the second degree; $f_{13}^{(k)}(z)$, $f_{23}^{(k)}(z)$ are third degree polynomials [27].

With approximation (1.1), the components of the strain tensor of the layer are defined by

$$e_{11}^{(k)}=\frac{\partial U_{1l}^{(k)}}{\partial x}f_{1l}^{(k)},\qquad e_{22}^{(k)}=\frac{\partial U_{2l}^{(k)}}{\partial y}f_{2l}^{(k)},\qquad e_{33}^{(k)}=W_p^{(k)}\frac{\partial\beta_p^{(k)}}{\partial z},$$

$$2e_{12}^{(k)} = \frac{\partial U_{1l}^{(k)}}{\partial y} f_{1l}^{(k)} + \frac{\partial U_{2l}^{(k)}}{\partial x} f_{2l}^{(k)}, \quad 2e_{13}^{(k)} = U_{1l}^{(k)} \frac{\partial f_{1l}^{(k)}}{\partial z} + \frac{\partial W_p^{(k)}}{\partial x} \beta_p^{(k)},$$

$$2e_{23}^{(k)} = U_{2l}^{(k)} \frac{\partial f_{2l}^{(k)}}{\partial z} + \frac{\partial W_p^{(k)}}{\partial y} \beta_p^{(k)}. \tag{1.2}$$

The expressions for the stresses can be derived from Hooke's law and formulas (1.2):

$$\sigma_{11}^{(k)} = C_{11}^{(k)} \frac{\partial U_{1l}^{(k)}}{\partial x} f_{1l}^{(k)} + C_{12}^{(k)} \frac{\partial U_{2l}^{(k)}}{\partial y} f_{2l}^{(k)} + C_{13}^{(k)} W_p^{(k)} \frac{\partial \beta_p^{(k)}}{\partial z},$$

$$\sigma_{22}^{(k)} = C_{21}^{(k)} \frac{\partial U_{1l}^{(k)}}{\partial x} f_{1l}^{(k)} + C_{22}^{(k)} \frac{\partial U_{2l}^{(k)}}{\partial y} f_{2l}^{(k)} + C_{23}^{(k)} W_p^{(k)} \frac{\partial \beta_p^{(k)}}{\partial z},$$

$$\sigma_{33}^{(k)} = C_{31}^{(k)} \frac{\partial U_{1l}^{(k)}}{\partial x} f_{1l}^{(k)} + C_{32}^{(k)} \frac{\partial U_{2l}^{(k)}}{\partial y} f_{2l}^{(k)} + C_{33}^{(k)} W_p^{(k)} \frac{\partial \beta_p^{(k)}}{\partial z},$$

$$\sigma_{12}^{(k)} = G_{12}^{(k)} \left(\frac{\partial U_{1l}^{(k)}}{\partial y} f_{1l}^{(k)} + \frac{\partial U_{2l}^{(k)}}{\partial x} f_{2l}^{(k)} \right),$$

$$\sigma_{13}^{(k)} = G_{13}^{(k)} \left(U_{1l}^{(k)} \frac{\partial f_{1l}^{(k)}}{\partial z} + \frac{\partial W_p^{(k)}}{\partial x} \beta_p^{(k)} \right),$$

$$\sigma_{23}^{(k)} = G_{23}^{(k)} \left(U_{2l}^{(k)} \frac{\partial f_{2l}^{(k)}}{\partial z} + \frac{\partial W_p^{(k)}}{\partial y} \beta_p^{(k)} \right). \tag{1.3}$$

With (1.2) and (1.3), the variation of the potential strain energy takes the form

$$\begin{aligned}
\delta\Pi = \iint_s \int_{a_{k-1}}^{a_k} \int_{t_1}^{t_2} \Bigg\{ & \left[C_{11}^{(k)} \frac{\partial U_{1l}^{(k)}}{\partial x} f_{1l}^{(k)} + C_{12}^{(k)} \frac{\partial U_{2l}^{(k)}}{\partial y} f_{2l}^{(k)} + C_{13}^{(k)} W_p^{(k)} \frac{\partial \beta_p^{(k)}}{\partial z} \right] \delta \frac{\partial U_{1\bar{l}}^{(k)}}{\partial x} f_{1\bar{l}}^{(k)} \\
& + \left[C_{21}^{(k)} \frac{\partial U_{1l}^{(k)}}{\partial x} f_{1l}^{(k)} + C_{22}^{(k)} \frac{\partial U_{2l}^{(k)}}{\partial y} f_{2l}^{(k)} + C_{23}^{(k)} W_p^{(k)} \frac{\partial \beta_p^{(k)}}{\partial z} \right] \delta \frac{\partial U_{2\bar{l}}^{(k)}}{\partial x} f_{2\bar{l}}^{(k)} \\
& + \left[C_{31}^{(k)} \frac{\partial U_{1l}^{(k)}}{\partial x} f_{1l}^{(k)} + C_{32}^{(k)} \frac{\partial U_{2l}^{(k)}}{\partial y} f_{2l}^{(k)} + C_{33}^{(k)} W_p^{(k)} \frac{\partial \beta_p^{(k)}}{\partial z} \right] \delta W_{\bar{p}}^{(k)} \frac{\partial \beta_{\bar{p}}^{(k)}}{\partial z} \\
& + \left[G_{12}^{(k)} \left(\frac{\partial U_{1l}^{(k)}}{\partial y} f_{1l}^{(k)} + \frac{\partial U_{2l}^{(k)}}{\partial x} f_{2l}^{(k)} \right] \delta \left(\frac{\partial U_{1\bar{l}}^{(k)}}{\partial y} f_{1\bar{l}}^{(k)} + \frac{\partial U_{2\bar{l}}^{(k)}}{\partial x} f_{2\bar{l}}^{(k)} \right) \right. \\
& + \left[G_{13}^{(k)} \left(U_{1l}^{(k)} \frac{\partial f_{1l}^{(k)}}{\partial z} + \frac{\partial W_p^{(k)}}{\partial x} \beta_p^{(k)} \right) \right] \delta \left(U_{1\bar{l}}^{(k)} \frac{\partial f_{1\bar{l}}^{(k)}}{\partial z} + \frac{\partial W_{\bar{p}}^{(k)}}{\partial x} \beta_{\bar{p}}^{(k)} \right) \\
& + \left[G_{23}^{(k)} \left(U_{2l}^{(k)} \frac{\partial f_{2l}^{(k)}}{\partial z} + \frac{\partial W_p^{(k)}}{\partial y} \beta_p^{(k)} \right) \right] \delta \left(U_{2\bar{l}}^{(k)} \frac{\partial f_{2\bar{l}}^{(k)}}{\partial z} + \frac{\partial W_{\bar{p}}^{(k)}}{\partial y} \beta_{\bar{p}}^{(k)} \right) \Bigg\} dt dz dS.
\end{aligned} \tag{1.4}$$

The variation of the kinetic energy can be written as follows:

$$\delta T^{(k)} = -\iint\limits_{S} \int\limits_{a_{k-1}}^{a_k} \rho^{(k)} \left\{ \int\limits_{t_1}^{t_2} \left[(\ddot{U}_{1l}^{(k)} f_{1l}^{(k)}) \delta(U_{1\bar{l}}^{(k)} f_{1\bar{l}}^{(k)}) + (\ddot{U}_{2l}^{(k)} f_{2l}^{(k)}) \delta(U_{2\bar{l}}^{(k)} f_{2\bar{l}}^{(k)}) \right.\right.$$

$$\left. + (\ddot{W}_{p}^{(k)} \beta_{p}^{(k)}) \delta(W_{\bar{p}}^{(k)} \beta_{\bar{p}}^{(k)}) \right] dt - [(\dot{U}_{1l}^{(k)} f_{l}^{(k)}) \delta(U_{1\bar{l}}^{(k)} f_{\bar{l}}^{(k)}) + (\dot{U}_{2l}^{(k)} f_{l}^{(k)}) \delta(U_{2\bar{l}}^{(k)} f_{\bar{l}}^{(k)})$$

$$\left.\left. + (\dot{W}_{p}^{(k)} \beta_{p}^{(k)}) \delta(W_{\bar{p}}^{(k)} \beta_{\bar{p}}^{(k)})]\right|_{t_1}^{t_2} \right\} dz dS. \tag{1.5}$$

The unknown functions along the *X*-axis in plan of the structure are represented by linear, along the *Y*-axis, trigonometric functions:

$$U_{1l}^{(k)}(x, y, t) = (U_{1l1}^{(k)} f_{u1}^{(k)}(x) + U_{1l2}^{(k)} f_{u2}^{(k)}(x)) \sin \frac{\pi n y}{b} e^{-i\omega t},$$

$$U_{2l}^{(k)}(x, y, t) = (U_{2l1}^{(k)} f_{u1}^{(k)}(x) + U_{2l2}^{(k)} f_{u2}^{(k)}(x)) \cos \frac{\pi n y}{b} e^{-i\omega t},$$

$$W_{p}^{(k)}(x, y, t) = (W_{p1}^{(k)} f_{u1}^{(k)}(x) + W_{p2}^{(k)} f_{u2}^{(k)}(x)) \sin \frac{\pi n y}{b} e^{-i\omega t}, \tag{1.6}$$

where $f_{u1}(x) = 1 - x/L$, $f_{u2}(x) = x/L$; L is the length of the finite element along the *X*-axis; ω is the frequency of free vibrations.

The equations of motion of a finite element are obtained based on the following variational equation:

$$\delta \Pi - \delta T = 0. \tag{1.7}$$

Using expressions (1.4) and (1.5), approximation (1.6), and performing the appropriate transformations of Eq. (1.7), we obtain the algebraic equations of motion for a finite element

$$\int\limits_{0}^{L} \left[\left(B11_{\bar{l}l}^{(k)} \frac{\partial f_{u\bar{s}}(x)}{\partial x} \frac{\partial f_{us}(x)}{\partial x} + TU1_{\bar{l}l}^{(k)} f_{u\bar{s}}(x) f_{us}(x) + B611_{\bar{l}l}^{(k)} f_{u\bar{s}}(x) f_{us}(x) \left(\frac{\pi n}{b} \right)^2 \right) U_{1ls}^{(k)} \right.$$

$$+ \left(B612_{\bar{l}l}^{(k)} \frac{\partial f_{u\bar{s}}(x)}{\partial x} f_{us}(x) - B12_{\bar{l}l}^{(k)} f_{u\bar{s}}(x) \frac{\partial f_{us}(x)}{\partial x} \right) \left(\frac{\pi n}{b} \right) U_{2ls}^{(k)}$$

$$\left. + \left(CUW1_{\bar{l}p}^{(k)} \frac{\partial f_{us}(x)}{\partial x} f_{u\bar{s}}(x) + SD1_{\bar{l}p}^{(k)} f_{us}(x) \frac{\partial f_{u\bar{s}}(x)}{\partial x} \right) W_{ps}^{(k)} - \omega^2 BT1_{\bar{l}l}^{(k)} f_{u\bar{s}}(x) f_{us}(x) U_{1ls}^{(k)} \right] dx = 0,$$

$$\int\limits_{0}^{L} \left[\left(B612_{\bar{l}l}^{(k)} \frac{\partial f_{u\bar{s}}(x)}{\partial x} f_{us}(x) - B12_{\bar{l}l}^{(k)} f_{u\bar{s}}(x) \frac{\partial f_{us}(x)}{\partial x} \right) \left(\frac{\pi n}{b} \right) U_{1ls}^{(k)} \right.$$

$$+ \left(B22_{\bar{l}l}^{(k)} f_{u\bar{s}}(x) f_{us}(x) \left(\frac{\pi n}{b} \right)^2 + TU2_{\bar{l}l}^{(k)} f_{u\bar{s}}(x) f_{us}(x) + B622_{\bar{l}l}^{(k)} \frac{\partial f_{u\bar{s}}(x)}{\partial x} \frac{\partial f_{us}(x)}{\partial x} \right) U_{2ls}^{(k)}$$

$$\left. + (CUW2_{\bar{l}p}^{(k)} - SD2_{\bar{l}p}^{(k)}) \left(\frac{\pi n}{b} \right) f_{u\bar{s}}(x) f_{ws}(x) W_{ps}^{(k)} - \omega^2 BT2_{\bar{l}l}^{(k)} f_{u\bar{s}}(x) f_{us}(x) U_{2ls}^{(k)} \right] dx = 0,$$

$$\int\limits_{0}^{L} \left[\left(SD1_{\bar{p}l}^{(k)} f_{w\bar{s}}(x) \frac{\partial f_{us}(x)}{\partial x} + CUW1_{\bar{p}l}^{(k)} \frac{\partial f_{u\bar{s}}(x)}{\partial x} f_{us}(x) \right) U_{1ls}^{(k)} \right.$$

$$+(CUW2_{\bar{p}l}^{(k)} - SD2_{\bar{p}l}^{(k)})\left(\frac{\pi n}{b}\right) f_{u\bar{s}}(x) f_{us}(x) U_{2ls}^{(k)}$$

$$+\left(\left(CC2_{\bar{p}p}^{(k)}\left(\frac{\pi n}{b}\right)^2 + ZZ_{\bar{p}p}^{(k)}\right) f_{w\bar{s}}(x) f_{ws}(x) + CC1_{\bar{p}p}^{(k)} \frac{df_{w\bar{s}}(x)}{dx}\frac{df_{ws}(x)}{dx}\right) W_{ps}^{(k)}$$

$$-\omega^2 ZT_{\bar{p}p}^{(k)} f_{w\bar{s}}(x) f_{ws}(x) W_{ps}^{(k)}\Bigg] dx = 0. \tag{1.8}$$

The system of algebraic equations of equilibrium of a finite element is written for the amplitudes of tangential displacements along the *X*-axis on the outer surfaces of the layer at the nodes of the finite element ($U_{111}^{(k)}, U_{121}^{(k)}$ at the first node and $U_{112}^{(k)}, U_{122}^{(k)}$ at the second node); the amplitudes of tangential displacements along the *Y*-axis on the outer surfaces of the layer at the nodes of the finite element ($U_{211}^{(k)}, U_{221}^{(k)}$ at the first node and $U_{212}^{(k)}, U_{222}^{(k)}$ at the second node); the amplitudes of normal displacements at the nodes of the finite element ($W_{11}^{(k)}$, $W_{21}^{(k)}$ at the first node and $W_{12}^{(k)}$, $W_{22}^{(k)}$ at the second node); the amplitudes of shear functions along the *X*-axis ($U_{131}^{(k)}$ at the first node and $U_{132}^{(k)}$ at the second node); the amplitudes of shear functions along the *Y*-axis ($U_{231}^{(k)}$ at the first node and $U_{232}^{(k)}$ at the second node); the amplitudes of the compression functions ($W_{31}^{(k)}$ at the first node and $W_{32}^{(k)}$ at the second node). In general, for one element, we have a system of eighteen equations with eighteen unknowns. The location of the unknown nodal displacement amplitudes on the outer surfaces of the finite element allows the structure to be modeled not only in plan but also across the thickness.

The equation for the layer with boundary conditions has the following matrix form:

$$\begin{bmatrix} [k_{11}^{(k)}] & [k_{12}^{(k)}] & [k_{13}^{(k)}] \\ [k_{21}^{(k)}] & [k_{22}^{(k)}] & [k_{23}^{(k)}] \\ [k_{31}^{(k)}] & [k_{32}^{(k)}] & [k_{33}^{(k)}] \end{bmatrix} \begin{Bmatrix} \{v_1^{(k)}\} \\ \{v_2^{(k)}\} \\ \{v_3^{(k)}\} \end{Bmatrix} - \omega^2 \begin{bmatrix} [m_{11}^{(k)}] & [m_{12}^{(k)}] & [m_{13}^{(k)}] \\ [m_{21}^{(k)}] & [m_{22}^{(k)}] & [m_{23}^{(k)}] \\ [m_{31}^{(k)}] & [m_{32}^{(k)}] & [m_{33}^{(k)}] \end{bmatrix} \begin{Bmatrix} \{v_1^{(k)}\} \\ \{v_2^{(k)}\} \\ \{v_3^{(k)}\} \end{Bmatrix} = \begin{Bmatrix} \{0\} \\ \{0\} \\ \{0\} \end{Bmatrix}, \tag{1.9}$$

where $\{v_1^{(k)}\}$ are the displacement amplitudes on the upper surface of the layer; $\{v_2^{(k)}\}$ are the displacement amplitudes on the lower surface of the layer; $\{v_3^{(k)}\}$ are the amplitudes of the shear and compression functions.

The free vibrations of a three-layer plate will be analyzed below. For this case, the equations of free vibrations have the form

$$\begin{bmatrix} [k_{11}^{(1)}] & [k_{12}^{(1)}] & 0 & 0 & [k_{13}^{(1)}] & 0 & 0 \\ [k_{21}^{(1)}] & [k_{22}^{(1)}]+[k_{11}^{(2)}] & [k_{12}^{(2)}] & 0 & [k_{23}^{(1)}] & [k_{13}^{(2)}] & 0 \\ 0 & [k_{12}^{(2)}] & [k_{22}^{(2)}]+[k_{11}^{(3)}] & [k_{12}^{(3)}] & 0 & [k_{23}^{(2)}] & [k_{13}^{(3)}] \\ 0 & 0 & [k_{12}^{(3)}] & [k_{22}^{(3)}] & 0 & 0 & [k_{23}^{(3)}] \\ [k_{31}^{(1)}] & [k_{32}^{(1)}] & 0 & 0 & [k_{33}^{(1)}] & 0 & 0 \\ 0 & [k_{31}^{(2)}] & [k_{32}^{(2)}] & 0 & 0 & [k_{33}^{(2)}] & 0 \\ 0 & 0 & [k_{31}^{(3)}] & [k_{32}^{(3)}] & 0 & 0 & [k_{33}^{(3)}] \end{bmatrix}$$

$$-\omega^2\begin{bmatrix}
\left[m_{11}^{(1)}\right] & \left[m_{12}^{(1)}\right] & 0 & 0 & \left[m_{13}^{(1)}\right] & 0 & 0 \\
\left[m_{21}^{(1)}\right] & \left[m_{22}^{(1)}\right]+\left[m_{11}^{(2)}\right] & \left[m_{12}^{(2)}\right] & 0 & \left[m_{23}^{(1)}\right] & \left[m_{13}^{(2)}\right] & 0 \\
0 & \left[m_{12}^{(2)}\right] & \left[m_{22}^{(2)}\right]+\left[m_{11}^{(3)}\right] & \left[m_{12}^{(3)}\right] & 0 & \left[m_{23}^{(2)}\right] & \left[m_{13}^{(3)}\right] \\
0 & 0 & \left[m_{12}^{(3)}\right] & \left[m_{22}^{(3)}\right] & 0 & 0 & \left[m_{23}^{(3)}\right] \\
\left[m_{31}^{(1)}\right] & \left[m_{32}^{(1)}\right] & 0 & 0 & \left[m_{33}^{(1)}\right] & 0 & 0 \\
0 & \left[m_{31}^{(2)}\right] & \left[m_{32}^{(2)}\right] & 0 & 0 & \left[m_{33}^{(2)}\right] & 0 \\
0 & 0 & \left[m_{31}^{(3)}\right] & \left[m_{32}^{(3)}\right] & 0 & 0 & \left[m_{33}^{(3)}\right]
\end{bmatrix}=\begin{Bmatrix}0\\0\\0\\0\\0\\0\\0\end{Bmatrix}. \qquad (1.10)$$

Since the plate is divided into 100 finite elements, this problem has the following number of unknowns: $101(3 + 1)\times3 + 101\times3\times3 = 2121$. If there is a foundation modeled by a layer of finite thickness, the number of unknowns increases slightly: $101\times(4 + 1)\times3 + 101\times4\times3 = 2727$. The capabilities of modern computers, as well as the availability of standard software for solving Eqs. (1.10) allow us to solve this problem.

When a layer is divided into 64 sublayers, the number of unknowns increases significantly: $101\times(64\times3 + 1)\times3 + 101\times64\times3\times3 = 116655$; if there is a foundation, then $101\times(64\times4 + 1)\times3 + 101\times64\times4\times3 = 155439$. In this case, we use the following algorithm. We write Eqs. (1.9) for a sublayer as follows:

$$\begin{bmatrix}
\left[k_{11}^{(k)}\right]-\omega^2\left[m_{11}^{(k)}\right] & \left[k_{12}^{(k)}\right]-\omega^2\left[m_{12}^{(k)}\right] & \left[k_{13}^{(k)}\right]-\omega^2\left[m_{13}^{(k)}\right] \\
\left[k_{21}^{(k)}\right]-\omega^2\left[m_{21}^{(k)}\right] & \left[k_{22}^{(k)}\right]-\omega^2\left[m_{22}^{(k)}\right] & \left[k_{23}^{(k)}\right]-\omega^2\left[m_{23}^{(k)}\right] \\
\left[k_{31}^{(k)}\right]-\omega^2\left[m_{31}^{(k)}\right] & \left[k_{32}^{(k)}\right]-\omega^2\left[m_{32}^{(k)}\right] & \left[k_{33}^{(k)}\right]-\omega^2\left[m_{33}^{(k)}\right]
\end{bmatrix}\begin{Bmatrix}\{v_1^{(k)}\}\\\{v_2^{(k)}\}\\\{v_3^{(k)}\}\end{Bmatrix}=\begin{Bmatrix}\{0\}\\\{0\}\\\{0\}\end{Bmatrix}$$

or

$$\begin{bmatrix}
\left[K_{11}^{(k)}\right] & \left[K_{12}^{(k)}\right] & \left[K_{13}^{(k)}\right] \\
\left[K_{21}^{(k)}\right] & \left[K_{22}^{(k)}\right] & \left[K_{23}^{(k)}\right] \\
\left[K_{31}^{(k)}\right] & \left[k_{32}^{(k)}\right] & \left[k_{33}^{(k)}\right]
\end{bmatrix}\begin{Bmatrix}\{v_1^{(k)}\}\\\{v_2^{(k)}\}\\\{v_3^{(k)}\}\end{Bmatrix}=\begin{Bmatrix}\{0\}\\\{0\}\\\{0\}\end{Bmatrix}. \qquad (1.11)$$

The amplitudes of the shear analogs of the displacements of a layer are internal; they are not combined with other layers when designing a layered structure. They can be eliminated using a procedure similar to the well-known super-element technology. Let us write the vector of amplitudes of shear analogs of layer displacements using Eqs. (1.11):

$$\{v_3^{(k)}\}=-[K_{33}^{(k)}]^{-1}[K_{31}^{(k)}]\{v_1^{(k)}\}-[K_{33}^{(k)}]^{-1}[K_{32}^{(k)}]\{v_2^{(k)}\},$$

further, Eqs. (1.9) become:

$$\begin{bmatrix}
\left[\left[K_{11}^{(k)}\right]-\left[K_{13}^{(k)}\right]\left[K_{33}^{(k)}\right]^{-1}\left[K_{31}^{(k)}\right]\right] & \left[\left[K_{12}^{(k)}\right]-\left[K_{13}^{(k)}\right]\left[K_{33}^{(k)}\right]^{-1}\left[K_{32}^{(k)}\right]\right] \\
\left[\left[K_{21}^{(k)}\right]-\left[K_{23}^{(k)}\right]\left[K_{33}^{(k)}\right]^{-1}\left[K_{31}^{(k)}\right]\right] & \left[\left[K_{22}^{(k)}\right]-\left[K_{23}^{(k)}\right]\left[K_{33}^{(k)}\right]^{-1}\left[K_{32}^{(k)}\right]\right]
\end{bmatrix}\begin{Bmatrix}\{v_2^{(k)}\}\\\{v_2^{(k)}\}\end{Bmatrix}=\begin{Bmatrix}\{0\}\\\{0\}\end{Bmatrix}. \qquad (1.12)$$

Equations (1.12) can be written as follows:

$$\begin{bmatrix}
\left[\overline{K}_{11}^{(k)}\right] & \left[\overline{K}_{12}^{(k)}\right] \\
\left[\overline{K}_{21}^{(k)}\right] & \left[\overline{K}_{22}^{(k)}\right]
\end{bmatrix}\begin{Bmatrix}\{v_1^{(k)}\}\\\{v_2^{(k)}\}\end{Bmatrix}=\begin{Bmatrix}\{0\}\\\{0\}\end{Bmatrix}. \qquad (1.13)$$

Next, we consider two adjacent layers. The governing system of equilibrium equations for them has a form similar to (1.11), but now $\{v_3^{(k)}\}$ are the displacement amplitudes at the interface of the two layers under consideration. We reduce the displacements $\{v_3^{(k)}\}$, similarly to the above procedure. We repeat this until we get a system of equations of the following form:

$$\begin{bmatrix} [\widetilde{K}_{11}] & [\widetilde{K}_{12}] \\ [\widetilde{K}_{21}] & [\widetilde{K}_{22}] \end{bmatrix} \begin{Bmatrix} \{v_1\} \\ \{v_{n+1}\} \end{Bmatrix} = \begin{Bmatrix} \{0\} \\ \{0\} \end{Bmatrix}, \tag{1.14}$$

where $\{v_1^{(k)}\}$ are the displacement amplitudes on the upper surface of the layer stack; $\{v_{n+1}\}$ are the displacement amplitudes on the lower surface of the layer stack.

The frequencies of free vibrations are obtained from system (1.14) by the method of sequential refinement of the search interval, using as the frequencies obtained from Eqs. (1.10) as the initial one.

This approach significantly reduces the number of operations when solving the governing system of equations (operations with zeros are reduced substantially). Its benefits become especially obvious when the layer is divided into sublayers (2, 4, 8, 16, 32, 64, etc.), and also if the structure consists of mutually alternating identical layers with different directions. The results obtained are validated against the alternative calculation according to the method outlined below.

2. Version of the Semianalytical Finite-Element Method for Studying the Free Vibrations and Finding the Distribution of the Unknown Functions over the Thickness of the Structure Based on the Analytical Solution of the Corresponding System of Differential Equations (V2).

Let us introduce the following approximation of the unknown functions of displacements and stresses in the plan of a finite element:

$$U_1^{(k)}(x,y,z,t) = (\varphi_1(x,t)u_{11}^{(k)}(z) + \varphi_2(x,t)u_{12}^{(k)}(z))\sin\frac{\pi n y}{b},$$

$$U_2^{(k)}(x,y,z,t) = (\varphi_1(x,t)u_{21}^{(k)}(z) + \varphi_2(x,t)u_{22}^{(k)}(z))\cos\frac{\pi n y}{b},$$

$$U_3^{(k)}(x,y,z,t) = (\varphi_1(x,t)w_1^{(k)}(z) + \varphi_2(x,t)w_2^{(k)}(z))\sin\frac{\pi n y}{b},$$

$$\sigma_{13}^{(k)}(x,y,z,t) = (\varphi_1(x,t)\tau_{11}^{(k)}(z) + \varphi_2(x,t)\tau_{12}^{(k)}(z))\sin\frac{\pi n y}{b},$$

$$\sigma_{23}^{(k)}(x,y,z,t) = (\varphi_1(x,t)\tau_{21}^{(k)}(z) + \varphi_2(x,t)\tau_{22}^{(k)}(z))\cos\frac{\pi n y}{b},$$

$$\sigma_{33}^{(k)}(x,y,z,t) = (\varphi_1(x,t)\sigma_1^{(k)}(z) + \varphi_2(x,t)\sigma_2^{(k)}(z))\sin\frac{\pi n y}{b}, \tag{2.1}$$

where $\varphi_1(x,t) = e^{-i\omega t}(1 - x/L)$, $\varphi_2(x,t) = e^{-i\omega t}(x/L)$; L is the length of the finite element; $u_{11}^{(k)}(z)$, $u_{12}^{(k)}(z)$, $u_{21}^{(k)}(z)$, $u_{22}^{(k)}(z)$, $w_1^{(k)}(z)$, $w_2^{(k)}(z)$, $w^{(k)T} = \{w_1^{(k)}(z), w_2^{(k)}(z)\}$, $\tau_{21}^{(k)}(z)$, $\tau_{22}^{(k)}(z)$, $\sigma_1^{(k)}(z)$, $\sigma_2^{(k)}(z)$ are the unknown distribution functions of displacements and stresses over thickness at the nodes of the finite element.

Using expressions for displacements (2.1), we find the strains from the kinematic equations:

$$e_{11}^{(k)}(x,y,z,t) = \left(\frac{\partial\varphi_1(x,t)}{\partial x}u_{11}^{(k)}(z) + \frac{\partial\varphi_2(x,t)}{\partial x}u_{12}^{(k)}(z)\right)\sin\frac{\pi n y}{b},$$

$$e_{22}^{(k)}(x,y,z,t) = -\frac{\pi n}{b}(\varphi_1(x,t)u_{21}^{(k)}(z) + \varphi_2(x,\ t)u_{22}^{(k)}(z))\sin\frac{\pi n y}{b},$$

$$e_{33}^{(k)}(x,y,z,t)=\left(\varphi_1(x,t)\frac{\partial w_1^{(k)}(z)}{\partial z}+\varphi_2(x,t)\frac{\partial w_2^{(k)}(z)}{\partial z}\right)\sin\frac{\pi n y}{b},$$

$$2e_{23}^{(k)}(x,y,z,t)=\left(\varphi_1(x,t)\frac{\partial u_{21}^{(k)}(z)}{\partial z}+\varphi_2(x,t)\frac{\partial u_{22}^{(k)}(z)}{\partial z}\right.$$

$$\left.+\frac{\pi n}{b}(\varphi_1(x,t)w_1^{(k)}(z)+\varphi_2(x,t)w_2^{(k)}(z))\right)\cos\frac{\pi n y}{b},$$

$$2e_{13}^{(k)}(x,y,z,t)=\left(\varphi_1(x,t)\frac{\partial u_{11}^{(k)}(z)}{\partial z}+\varphi_2(x,t)\frac{\partial u_{12}^{(k)}(z)}{\partial z}\right.$$

$$\left.+\frac{\partial\varphi_1(x,t)}{\partial x}w_1^{(k)}(z)+\frac{\partial\varphi_2(x,t)}{\partial x}w_2^{(k)}(z)\right)\sin\frac{\pi n y}{b},$$

$$2e_{12}^{(k)}(x,y,z,t)=\left(\frac{\pi n}{b}\left(\varphi_1(x,t)u_{11}^{(k)}(z)+\varphi_2(x,t)u_{12}^{(k)}(z)\right)\right.$$

$$\left.+\frac{\partial\varphi_1(x,t)}{\partial x}u_{21}^{(k)}(z)+\frac{\partial\varphi_2(x,t)}{\partial x}u_{22}^{(k)}(z)\right)\cos\frac{\pi n y}{b}.$$

The stresses and strains are related by

$$\sigma_{11}^{(k)}=B_{11}^{(k)}e_{11}^{(k)}+B_{12}^{(k)}e_{22}^{(k)}+B_{13}^{(k)}\sigma_{33}^{(k)},\qquad \sigma_{22}^{(k)}=B_{21}^{(k)}e_{11}^{(k)}+B_{22}^{(k)}e_{22}^{(k)}+B_{23}^{(k)}\sigma_{33}^{(k)},$$

$$B_{33}^{(k)}\sigma_{33}^{(k)}=B_{13}^{(k)}e_{11}^{(k)}+B_{23}^{(k)}e_{22}^{(k)}+e_{33}^{(k)},$$

$$\sigma_{23}^{(k)}=G_{23}^{(k)}2e_{23}^{(k)},\qquad \sigma_{13}^{(k)}=G_{13}^{(k)}2e_{13}^{(k)},\qquad \sigma_{12}^{(k)}=G_{12}^{(k)}2e_{12}^{(k)}.$$

The governing system of equations and boundary conditions are derived using the variational equation:

$$\delta R^{(k)}-\delta T^{(k)}=0.$$

Here

$$\delta R^{(k)}=\iint_S\int_{a_{k-1}}^{a_k}\int_{t_1}^{t_2}\left\{\left[\left(B_{11}^{(k)}\left(\frac{\partial\varphi_1(x,t)}{\partial x}u_{11}^{(k)}(z)+\frac{\partial\varphi_2(x,t)}{\partial x}u_{12}^{(k)}(z)\right)\right.\right.$$

$$\left.\left.-B_{12}^{(k)}\frac{\pi n}{b}(\varphi_1(x,t)u_{21}^{(k)}(z)+\varphi_2(x,t)u_{22}^{(k)}(z))+B_{13}^{(k)}(\varphi_1(x,t)\sigma_1^{(k)}(z)+\varphi_2(x,t)\sigma_2^{(k)}(z))\right)\sin\frac{\pi n y}{b}\right]$$

$$\times\delta\left(\left(\frac{\partial\varphi_1(x,t)}{\partial x}u_{11}^{(k)}(z)+\frac{\partial\varphi_2(x,t)}{\partial x}u_{12}^{(k)}(z)\right)\sin\frac{\pi n y}{b}\right)$$

$$+\left[\left(B_{21}^{(k)}\left(\frac{\partial\varphi_1(x,t)}{\partial x}u_{11}^{(k)}(z)+\frac{\partial\varphi_2(x,t)}{\partial x}u_{12}^{(k)}(z)\right)-B_{22}^{(k)}\frac{\pi n}{b}(\varphi_1(x,\,t)u_{21}^{(k)}(z)+\varphi(x,\,t)u_{22}^{(k)}(z))\right.\right.$$

$$+B_{23}^{(k)}\left(\varphi_1(x,t)\sigma_1^{(k)}(z)+\varphi_2(x,t)\sigma_2^{(k)}(z)\right)\Big)\sin\frac{\pi ny}{b}\Big]$$

$$\times\delta\left(-\frac{\pi n}{b}(\varphi_1(x,t)u_{21}^{(k)}(z)+\varphi_2(x,t)u_{22}^{(k)}(z))\sin\frac{\pi ny}{b}\right)$$

$$+\Big[G_{12}^{(k)}\Big(\frac{\pi n}{b}\varphi_1(x,t)u_{11}^{(k)}(z)+\frac{\pi n}{b}\varphi_2(x,t)u_{12}^{(k)}(z)$$

$$+\frac{\partial\varphi_1(x,t)}{\partial x}u_{21}^{(k)}(z)+\frac{\partial\varphi_2(x,t)}{\partial x}u_{22}^{(k)}(z)\Big)\cos\frac{\pi ny}{b}\Big]$$

$$\times\delta\left(\left(\frac{\pi n}{b}\varphi_1(x,t)u_{11}^{(k)}(z)+\frac{\pi n}{b}\varphi_2(x,t)u_{12}^{(k)}(z)+\frac{\partial\varphi_1(x,t)}{\partial x}u_{21}^{(k)}(z)+\frac{\partial\varphi_2'(x,t)}{\partial x}u_{22}^{(k)}(z)\right)\cos\frac{\pi ny}{b}\right)$$

$$+\Big[(\varphi_1(x,t)\sigma_1^{(k)}(z)+\varphi_2(x,t)\sigma_2^{(k)}(z))\sin\frac{\pi ny}{b}\Big]\delta\left(\left(\varphi_1(x,t)\frac{\partial w_1^{(k)}(z)}{\partial z}+\varphi_2(x,t)\frac{\partial w_2^{(k)}(z)}{\partial z}\right)\sin\frac{\pi ny}{b}\right)$$

$$+\Big[\Big(B_{13}^{(k)}\Big(\frac{\partial\varphi_1(x,t)}{\partial x}u_{11}^{(k)}(z)+\frac{\partial\varphi_2(x,t)}{\partial x}u_{12}^{(k)}(z)\Big)-B_{23}^{(k)}\frac{\pi n}{b}(\varphi_1(x,t)u_{21}^{(k)}(z)+\varphi_2(x,t)u_{22}^{(k)}(z))$$

$$+\left(\varphi_1(x,t)\frac{\partial w_1^{(k)}(z)}{\partial z}+\varphi_2(x,t)\frac{\partial w_2^{(k)}(z)}{\partial z}\right)-B_{33}^{(k)}(\varphi_1(x,t)\sigma_1^{(k)}(z)+\varphi_2(x,t)\sigma_2^{(k)}(z))\sin\frac{\pi ny}{b}\Big]$$

$$\times\delta\left((\varphi_1(x,t)\sigma_1^{(k)}(z)+\varphi_2(x,t)\sigma_2^{(k)}(z))\sin\frac{\pi ny}{b}\right)$$

$$+\Big[(\varphi_1(x,t)\tau_{21}^{(k)}(r)+\varphi_2(x,t)\tau_{22}^{(k)}(r))\cos\frac{\pi ny}{b}\Big]\delta\Big(\varphi_1(x,t)\frac{\partial u_{21}^{(k)}(z)}{\partial z}+\varphi_2(x,t)\frac{\partial u_{22}^{(k)}(z)}{\partial z}$$

$$+\frac{\pi n}{b}(\varphi_1(x,t)w_1^{(k)}(z)+\varphi_2(x,t)w_2^{(k)}(z))\cos\frac{\pi ny}{b}\Big)$$

$$+\Big[\Big(\varphi_1(x,t)\frac{\partial u_{21}^{(k)}(z)}{\partial z}+\varphi_2(x,t)\frac{\partial u_{22}^{(k)}(z)}{\partial z}+\frac{\pi n}{b}\varphi_1(x,t)w_1^{(k)}(z)+\frac{\pi n}{b}\varphi_2(x,t)w_2^{(k)}(z)$$

$$-\Big(\varphi_1(x,t)\tau_{21}^{(k)}(z)+\varphi_2(x,t)\tau_{22}^{(k)}(z)\Big)/G_{23}^{(k)}\Big)\cos\frac{\pi ny}{b}\Big]$$

$$\times\delta\left((\varphi_1(x,t)\tau_{21}^{(k)}(z)+\varphi_2(x,t)\tau_{22}^{(k)}(z))\cos\frac{\pi ny}{b}\right)$$

$$+\Big[(\varphi_1(x,t)\tau_{11}^{(k)}(z)+\varphi_2(x)\tau_{12}^{(k)}(z))\sin\frac{\pi ny}{b}\Big]\delta\Big(\varphi_1(x,t)\frac{\partial u_{11}^{(k)}(z)}{\partial z}+\varphi_2(x,t)\frac{\partial u_{12}^{(k)}(z)}{\partial z}$$

$$+\frac{\partial\varphi_1(x)}{\partial x}w_1^{(k)}(z)+\frac{\partial\varphi_2(x)}{\partial x}w_2^{(k)}(z)\Big)\sin\frac{\pi ny}{b}$$

$$+\Bigg[(\varphi_1(x,t)\frac{\partial u_{11}^{(k)}(z)}{\partial z}+\varphi_2(x,t)\frac{\partial u_{12}^{(k)}(z)}{\partial z}+\frac{\partial\varphi_1(x,t)}{\partial x}w_1^{(k)}(z)+\frac{\partial\varphi_2(x,t)}{\partial x}w_2^{(k)}(z)$$

$$-(\varphi_1(x,t)\tau_{11}^{(k)}(z)+\varphi_2(x,t)\tau_{12}^{(k)}(z))/G_{13}^{(k)}\Big)\sin\frac{\pi ny}{b}\Bigg]$$

$$\times\delta\left((\varphi_1(x,t)\tau_{11}^{(k)}(z)+\varphi_2(x,t)\tau_{12}^{(k)}(z))\sin\frac{\pi ny}{b}\right)\Bigg\}dtdzdS$$

is the variation of the Reissner functional

$$\delta T^{(k)}=-\iint\limits_S\int\limits_{a_{k-1}}^{a_k}\Bigg\{\int\limits_{t_1}^{t_2}\Bigg[\Bigg(\left(\frac{\partial^2\varphi_1(x,t)}{\partial t^2}u_{11}^{(k)}(z)+\frac{\partial^2\varphi_2(x,t)}{\partial t^2}u_{12}^{(k)}(z)\right)\sin\frac{\pi ny}{b}\Bigg)$$

$$\times\delta\left((\varphi_1(x,t)u_{11}^{(k)}(z)+\varphi_2(x,t)u_{12}^{(k)}(z))\sin\frac{\pi ny}{b}\right)$$

$$+\left(\left(\frac{\partial^2\varphi_1(x,t)}{\partial t^2}u_{21}^{(k)}(z)+\frac{\partial^2\varphi_2(x,t)}{\partial t^2}u_{22}^{(k)}(z)\right)\cos\frac{\pi ny}{b}\right)$$

$$\times\delta\left((\varphi_1(x,t)u_{21}^{(k)}(z)+\varphi_2(x,t)u_{22}^{(k)}(z))\cos\frac{\pi ny}{b}\right)$$

$$+\left(\left(\frac{\partial^2\varphi_1(x,t)}{\partial t^2}w_1^{(k)}(z)+\frac{\partial^2\varphi_2(x,t)}{\partial t^2}w_2^{(k)}(z)\right)\sin\frac{\pi ny}{b}\right)$$

$$\times\delta\left((\varphi_1(x,t)w_1^{(k)}(z)+\varphi_2(x,t)w_2^{(k)}(z))\sin\frac{\pi ny}{b}\right)\Bigg]dt$$

$$+\rho^{(k)}\Bigg[\Bigg(\left(\frac{\partial\varphi_1(x,t)}{\partial t}u_{11}^{(k)}(z)+\frac{\partial\varphi_2(x,t)}{\partial t}u_{12}^{(k)}(z)\right)\sin\frac{\pi ny}{b}\Bigg)$$

$$\times\delta\left((\varphi_1(x,t)u_{11}^{(k)}(z)+\varphi_2(x,t)u_{12}^{(k)}(z))\sin\frac{\pi ny}{b}\right)$$

$$+\left(\left(\frac{\partial\varphi_1(x,t)}{\partial t}u_{21}^{(k)}(z)+\frac{\partial\varphi_2(x,t)}{\partial t}u_{22}^{(k)}(z)\right)\cos\frac{\pi ny}{b}\right)$$

$$\times\delta\left((\varphi_1(x,t)u_{21}^{(k)}(z)+\varphi_2(x,t)u_{22}^{(k)}(z))\cos\frac{\pi ny}{b}\right)$$

$$+\left(\left(\frac{\partial\varphi_1(x,t)}{\partial t}(w_1^{(k)}(z)+\frac{\partial\varphi_2(x,t)}{\partial t}w_2^{(k)}(z)\right)\sin\frac{\pi ny}{b}\right)$$

$$\times\delta\left((\varphi_1(x,t)w_1^{(k)}(z)+\varphi_2(x,t)w_2^{(k)}(z))\sin\frac{\pi ny}{b}\right)\Bigg]\Bigg|_{t_1}^{t_2}\Bigg\}dzdS$$

is the variation of the kinetic energy.

The governing system of equations for one finite element is

$$\left(\begin{bmatrix} 0 & 0 & -k_{01} & \frac{1}{G_{13}^{(k)}}k_{00} & 0 & 0 \\ 0 & 0 & -\frac{\pi n}{b}k_{00} & 0 & \frac{1}{G_{23}^{(k)}}k_{00} & 0 \\ -B_{15}^{(k)}k_{00} & \frac{\pi n}{b}B_{25}^{(k)}k_{00} & 0 & 0 & 0 & B_{33}^{(k)}k_{00} \\ B_{11}^{(k)}k_{11}+\left(\left(\frac{\pi n}{b}\right)^2 G_{12}^{(k)}-\rho^{(k)}\omega^2\right)k_{00} & \frac{\pi n}{b}(B_{66}^{(k)}k_{01}-B_{12}^{(k)}k_{10}) & 0 & 0 & 0 & B_{13}^{(k)}k_{10} \\ \frac{\pi n}{b}(B_{66}^{(k)}k_{01}-B_{12}^{(k)}k_{10}) & G_{12}^{(k)}k_{11}+\left(\left(\frac{\pi n}{b}\right)^2 B_{22}^{(k)}-\rho^{(k)}\omega^2\right)k_{00} & 0 & 0 & 0 & -\frac{\pi n}{b}B_{23}^{(k)}k_{00} \\ 0 & 0 & -\rho^{(k)}\omega^2 k_{00} & k_{10} & \frac{\pi n}{b}k_{00} & 0 \end{bmatrix}\right.$$

$$\left.-\begin{bmatrix} k_{00}\frac{\partial}{\partial z} & 0 & 0 & 0 & 0 & 0 \\ 0 & k_{00}\frac{\partial}{\partial z} & 0 & 0 & 0 & 0 \\ 0 & 0 & k_{00}\frac{\partial}{\partial z} & 0 & 0 & 0 \\ 0 & 0 & 0 & k_{00}\frac{\partial}{\partial z} & 0 & 0 \\ 0 & 0 & 0 & 0 & k_{00}\frac{\partial}{\partial z} & 0 \\ 0 & 0 & 0 & 0 & 0 & k_{00}\frac{\partial}{\partial z} \end{bmatrix}\right)\begin{bmatrix} u_1^{(k)}(z) \\ u_2^{(k)}(z) \\ w^{(k)}(z) \\ \tau_1^{(k)}(z) \\ \tau_2^{(k)}(z) \\ \sigma^{(k)}(z) \end{bmatrix}=\begin{bmatrix} 0 \\ 0 \\ 0 \\ 0 \\ 0 \\ 0 \end{bmatrix}. \tag{2.2}$$

Here

$$k_{00}=\begin{bmatrix} l/3 & l/6 \\ l/6 & l/3 \end{bmatrix},\quad k_{10}=\begin{bmatrix} -1/2 & -1/2 \\ 1/2 & 1/2 \end{bmatrix},\quad k_{11}=\begin{bmatrix} 1/l & -1/l \\ -1/l & 1/l \end{bmatrix},$$

$$k_{01}=k_{10}^T,\quad u_1^{(k)T}=\{u_{11}^{(k)}(z),\ u_{12}^{(k)}(z)\},\quad u_2^{(k)T}=\{u_{21}^{(k)}(z),\ u_{22}^{(k)}(z)\},$$

$$w^{(k)T}=\{w_1^{(k)}(z),\ w_2^{(k)}(z)\},\quad \tau_1^{(k)T}=\{\tau_{11}^{(k)}(z),\ \tau_{12}^{(k)}(z)\},$$

$$\tau_2^{(k)T}=\{\tau_{21}^{(k)}(z),\ \tau_{22}^{(k)}(z)\},\quad \sigma^{(k)T}=\{\sigma_1^{(k)}(z),\ \sigma_2^{(k)}(z)\}.$$

Next, using Eqs. (2.2), we set up the governing system of differential equations for a layer and kinematic boundary conditions:

$$\begin{bmatrix} 0 & 0 & -K_{01} & \frac{1}{G_{13}^{(k)}}K_{00} & 0 & 0 \\ 0 & 0 & -\frac{\pi n}{b}K_{00} & 0 & \frac{1}{G_{23}^{(k)}}K_{00} & 0 \\ -B_{15}^{(k)}K_{00} & \frac{\pi n}{b}B_{25}^{(k)}K_{00} & 0 & 0 & 0 & B_{33}^{(k)}K_{00} \\ B_{11}^{(k)}K_{11}+((\frac{\pi n}{b})^2 G_{12}^{(k)}-\rho^{(k)}\omega^2)K_{00} & \frac{\pi n}{b}(B_{66}^{(k)}K_{01}-B_{12}^{(k)}K_{10}) & 0 & 0 & 0 & B_{13}^{(k)}K_{10} \\ \frac{\pi n}{b}(B_{66}^{(k)}K_{01}-B_{12}^{(k)}K_{10}) & G_{12}^{(k)}K_{11}+((\frac{\pi n}{b})^2 B_{22}^{(k)}-\rho^{(k)}\omega^2)K_{00} & 0 & 0 & 0 & -\frac{\pi n}{b}B_{23}^{(k)}K_{00} \\ 0 & 0 & -\rho^{(k)}\omega^2 K_{00} & K_{10} & \frac{\pi n}{b}K_{00} & 0 \end{bmatrix}$$

$$\left[\begin{matrix} K_{00}\dfrac{\partial}{\partial z} & 0 & 0 & 0 & 0 & 0 \\ 0 & K_{00}\dfrac{\partial}{\partial z} & 0 & 0 & 0 & 0 \\ 0 & 0 & K_{00}\dfrac{\partial}{\partial z} & 0 & 0 & 0 \\ 0 & 0 & 0 & K_{00}\dfrac{\partial}{\partial z} & 0 & 0 \\ 0 & 0 & 0 & 0 & K_{00}\dfrac{\partial}{\partial z} & 0 \\ 0 & 0 & 0 & 0 & 0 & K_{00}\dfrac{\partial}{\partial z} \end{matrix}\right]\left[\begin{matrix} u_{1i}^{(k)}(z) \\ u_{2i}^{(k)}(z) \\ w_i^{(k)}(z) \\ \tau_{1i}^{(k)}(z) \\ \tau_{2i}^{(k)}(z) \\ \sigma_i^{(k)}(z) \end{matrix}\right] = \left[\begin{matrix} 0 \\ 0 \\ 0 \\ 0 \\ 0 \\ 0 \end{matrix}\right]. \qquad (2.3)$$

Here

$$\{u_{1i}^{(k)}(z)\}^T = \{\ldots,\ u_{1i}^{(k)}(z),\ldots\}, \quad \{u_{2i}^{(k)}(z)\}^T = \{\ldots,\ u_{2i}^{(k)}(z),\ldots\},$$

$$\{w_i^{(k)}(z)\}^T = \{\ldots,\ w_i^{(k)}(z),\ldots\}, \quad \{\tau_{1i}^{(k)}(z)\}^T = \{\ldots,\ \tau_{1i}^{(k)}(z),\ldots\},$$

$$\{\tau_{1i}^{(k)}(z)\}^T = \{\ldots,\ \tau_{1i}^{(k)}(z),\ldots\}, \quad \{\sigma_{2i}^{(k)}(z)\}^T = \{\ldots,\ \sigma_{2i}^{(k)}(z),\ldots\},$$

where i is the number of the point at which the unknown functions are determined.

The vector of unknown functions is represented as

$$\left[\begin{matrix} \{u_{1i}^{(k)}\} \\ \{u_{2i}^{(k)}\} \\ \{w_i^{(k)}\} \\ \{\tau_{1i}^{(k)}\} \\ \{\tau_{2i}^{(k)}\} \\ \{\sigma_i^{(k)}\} \end{matrix}\right] = \left[\begin{matrix} \mu_{i1}^{(k)}(1) & \ldots, & \mu_{i1}^{(k)}(j) & \ldots, & \mu_{i1}^{(k)}(J) \\ \mu_{i2}^{(k)}(1) & \ldots, & \mu_{i2}^{(k)}(j) & \ldots, & \mu_{i2}^{(k)}(J) \\ \mu_{i3}^{(k)}(1) & \ldots, & \mu_{i3}^{(k)}(j) & \ldots, & \mu_{i3}^{(k)}(J) \\ \mu_{i4}^{(k)}(1) & \ldots, & \mu_{i4}^{(k)}(j) & \ldots, & \mu_{i4}^{(k)}(J) \\ \mu_{i5}^{(k)}(1) & \ldots, & \mu_{i5}^{(k)}(j) & \ldots, & \mu_{i5}^{(k)}(J) \\ \mu_{i6}^{(k)}(1) & \ldots, & \mu_{i6}^{(k)}(j) & \ldots, & \mu_{i6}^{(k)}(J) \end{matrix}\right]\left[C^{(k)}\right],$$

where $[C^{(k)}]^T = [C_1^{(k)} e^{z\beta_1^{(k)}}, \ldots, C_j^{(k)} e^{z\beta^{(k)}}, \ldots C_J^{(k)} e^{z\beta_J^{(k)}}]$, $\beta_j^{(k)}$ are the roots of the characteristic equation of the governing system of differential equations, which can be complex; $\mu_{i1}^{(k)}(j), \mu_{i2}^{(k)}(j), \mu_{i3}^{(k)}(j), \mu_{i4}^{(k)}(j), \mu_{i5}^{(k)}(j), \mu_{i6}^{(k)}(j)$ are its eigenvectors; $C_j^{(k)}$ are the constants of integration determined from the interface conditions between the layers and the boundary conditions on the outside surfaces at each node of the finite-element partition of the structure; J is the total number of required functions in the layer. The frequencies of free vibrations are determined by the method of sequential refinement of the search interval. The frequencies obtained by the model with polynomial approximation of the unknown functions over the thickness of the structure are used as the initial frequencies.

3. Numerical Results. The proposed models were tested for the case of hinged boundary by comparing the results obtained using the proposed methods and the analytical model [26, 29]. A good agreement of the calculation results was obtained. To make the article shorter, such a calculation is not presented.

Let us consider the free vibrations of a three-layer plate with composite layers with the following physical and mechanical characteristics: $E_1^{(1)}/E_2^{(1)} = 25/1$, $E_2^{(1)} = E_3^{(1)}$, $G_{12}^{(1)}/E_3^{(1)} = 0.5/1$, $G_{23}^{(1)}/E_3^{(1)} = 0.2/1$, $G_{13}^{(1)} = G_{12}^{(1)}$, $\nu_{12}^{(1)} = \nu_{13}^{(1)} = \nu_{23}^{(1)} = 0.25, \rho^{(1)} = \rho^{(2)} = \rho^{(3)} = \rho$. The second layer is rotated 90°. The thickness of the second layer is equal to the sum of the equal thicknesses of the outer layers.

The plate is square in plan $a = b = L$ with $L/h = 5$. The boundary $Y = 0, Y = b$ is hinged-movable; and the boundary $X = 0, X = a$ is free (such a description is often found in design models of bridge structures). The calculations were carried out

TABLE 1

$\overline{\omega}^2 = \omega^2(\rho h^2 / E_3^{(1)})$			
Frequency number	V1 model; each layer considered within one sublayer	V1 model; each layer is divided into 64 sublayers	V2 model
1	3.39394e-002	3.38903e-002	3.38885e-002
2	5.16716e-002	5.13323e-002	5.13305e-002
3	1.705426e-001	1.69176e-001	1.69176e-001

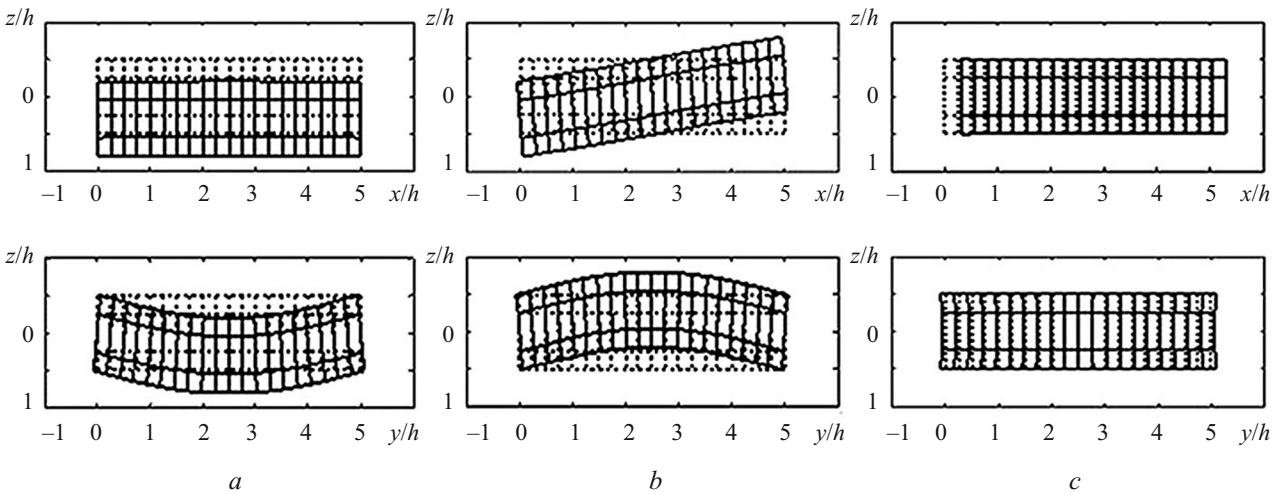

Fig. 1

using the proposed semianalytical methods with a polynomial approximation of the unknown functions over the thickness of the plate (V1) and with their analytical determination (V2). In the X-direction, the plate was divided into 100 elements.

Table 1 shows the three lowest vibration frequencies of the plate with free outer surfaces. They occur when $n = 1$ in approximation (1.6) ($\pi ny / b$).

Figure 1 shows their shapes in such vibrations. (It is very important to consider not only the frequencies but also the modes of free vibrations. In particular, in [27] it was shown that the dynamic coefficient of forced vibrations is strongly dependent not only on the closeness of the frequencies of free and forced vibrations but also on the closeness between the mode of displacement distribution under static load and displacement distribution at the frequency of free vibration). The left parts of the figure show the displacements for $Y = b / 2$, and the right parts of the figure show the displacements for $X = a$. The maximum displacement in the figures is equal to $h \times 0.3$.

The plate undergoes transverse bending vibrations at the first frequency, torsional vibrations at the second frequency, and bending vibrations in plan at the third frequency. The results obtained with the two methods considered are in good agreement. To obtain reliable results with the V1 model, it is sufficient to consider one sublayer to calculate the frequencies and to determine the displacement distribution.

The calculation according to the V1 model with the division of each layer into 64 sublayers and according to the V2 model was performed by the method of successive refinement of the search interval using the frequencies obtained with the V1 model as the initial frequencies, considering each layer within one sublayer. The figures for the three calculation options do not differ. When dividing each layer into 64 sublayers, the results of the V1 model tend to the results of the V2 model. They practically do not differ (coincide in four significant digits), which is an indirect confirmation of their reliability

TABLE 2

$\overline{\omega}^2 = \omega^2(\rho h^2 / E_3^{(1)})$			
Frequency number	V1 model; each layer is considered within one sublayer	V1 model; each layer is divided into 64 sublayers	V2 model
1	8.24258e-001	8.04085e-001	8.03912e-001
2	1.38257e+000	1.35819e+000	1.35801e+000
3	2.32489e+000	2.29406e+000	2.29387e+000

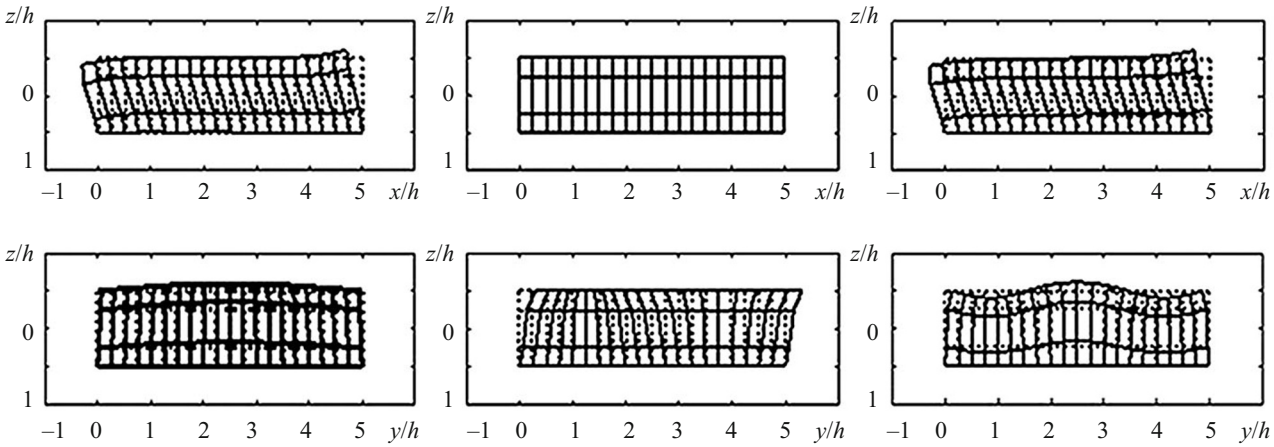

a *b* *c*

Fig. 2

Table 2 shows the results for the same structure, but with forbidden displacements on the lower surface (the design model of the pavement on bridges and rocks).

Figure 2 shows the modes of such vibrations. Vibrations at the first lowest frequency occur when $n = 1$, at the second frequency when $n = 2$, and at the third when $n = 3$. At the first and third frequencies, the structure swings in plan along the axis X with a slight bend. At the second frequency, the plate performs purely planar vibrations along the axis Y. While the calculation error for the V1 model with consideration of each layer within one sublayer did not exceed one percent, in this case it is slightly higher but quite acceptable. The results obtained with the V1 model with each layer divided into 64 sublayers and with the V2 model are in good agreement, which confirms the reliability of the results obtained.

Table 3 shows the three lowest frequencies of free vibrations of the plate on an elastic foundation modeled by a layer of finite thickness with the following physical and mechanical characteristics: $E^{(4)} = E_3^{(1)}/6.07$, $\nu^{(4)} = 0.25$, $\rho^{(4)} = \rho$. The thickness of the foundation is equal to the thickness of the plate. The bottom surface of the foundation is clamped.

Figure 3 shows the modes of such vibrations (they occur when $n = 1$).

A feature of this structure is that the first two frequencies differ slightly. When such a plate vibrates without a foundation (first example), the plate performs bending vibrations at the first lower frequency and torsional vibrations at the second frequency. In this case, torsional vibrations take the first place, bending vibrations come second. At the third frequency, torsional vibrations occur, but with the opposite sway of the plate in plan compared to the vibrations at the first frequency. The error of the V1 model with each layer and foundation considered within one sublayer is higher than in the previous cases, but it can be considered acceptable in engineering calculations. The results obtained with the V1 and V2 models practically coincides, which confirms their reliability.

TABLE 3

$\overline{\omega}^2 = \omega^2(\rho h^2 / E_3^{(1)})$			
Frequency number	V1 model; each layer is considered within one sublayer	V1 model; each layer is divided into 64 sublayers	V2 model
1	1.67454e-001	1.60512e-001	1.60498e-001
2	1.72637e-001	1.61355e-001	1.61345e-001
3	2.08077e-001	1.89205e-001	1.89189e-001

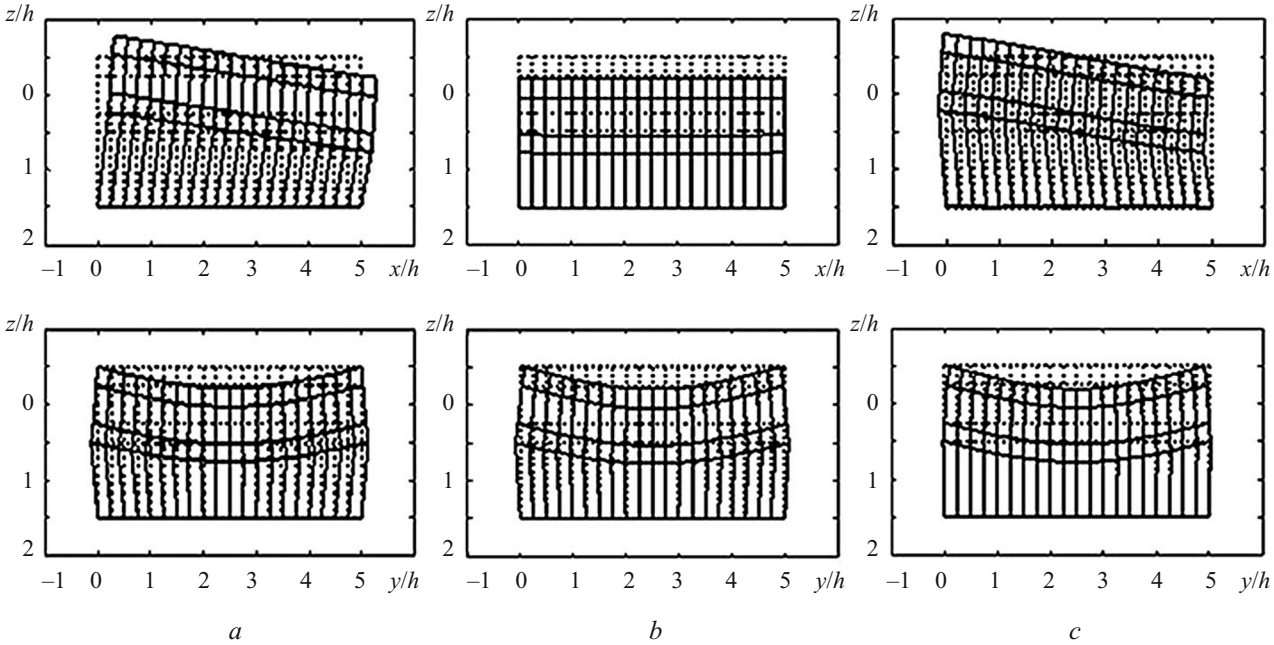

Fig. 3

To justify the need to take into account the inertial properties of the foundation in dynamic problems, we perform a calculation using the V1 model and considering each layer within one sublayer for $\rho^{(4)} = 0$. The square of the first frequency of free vibrations $\overline{\omega}^2 = \omega^2(\rho h^2 / E_3^{(1)})$ is 2.07700e-001 $(\text{Hz})^2$. The plate performs torsional vibrations. The square of the second frequency of free vibrations is 2.26554e-001 $(\text{Hz})^2$. At this frequency, the plate performs bending vibrations. At the third frequency ($\overline{\omega}^2$ = 2.88945e-001$(\text{Hz})^2$), the plate performs torsional vibrations. Neglecting the inertial properties of the foundation can significantly overestimate the squares of the lowest natural frequencies (compare with the second column of Table 3).

Conclusions. We have developed two versions of the semianalytical finite-element method for studying the free vibrations of layered composite plates. The lower surface of the plate can be free, clamped, and rest on a layer of finite thickness. Both approaches have their advantages and disadvantages. They are quite accurate. The disadvantages (a significant number of stiffness characteristics and a high order of the governing equations in the case of polynomial approximation in thickness and the need to find the roots of the characteristic system of equations and its eigenvectors in the case of the analytical determination of the unknown functions along the thickness of the plate) are insignificant due to the capabilities of modern computer technology. In the model with polynomial approximation of the unknown functions over the thickness of the structure, when each layer is divided into 64 sublayers and in the model with analytical determination of the unknown functions over the thickness, the

frequencies of free vibration are found by the method of sequential refinement of the search interval, with the determination of the initial frequencies from the model with polynomial approximation of the unknown functions over the thickness when each layer is considered within one layer. These approaches complement each other, contributing to the reliability of the results. The studies show that to achieve acceptable accuracy of the first version of the semianalytical finite-element method, it is sufficient to consider each layer within one sublayer, the frequencies and displacement distributions in such vibrations are acceptable. An attempt to design the plate on a foundation neglecting its inertial properties led to unacceptable results.

REFERENCES

1. V. A. Bazhenov, O. I. Gulyar, O. S. Sakharov, and I. I. Solodei, *Semianalytic Finite-Element Method in Problems of the Dynamics of Solids* [in Ukrainian], Kyiv (2012).
2. Ya. M. Grigorenko, E. I. Bespalova, A. B. Kitaigorodskii, and A. I. Shinkar', *Free Vibrations of Elements of Shell Structures* [in Russian], Naukova Dumka, Kyiv (1986).
3. Ya. M. Grigorenko, G. G. Vlaikov, and A. Ya. Grigorenko, *Numerical Analytic Solution of Shell Problems Based on Various Models* [in Russian], Akademperiodika, Kyiv (2006).
4. S. O. Papkov and V. V. Meleshko, "Flexural vibrations of a rectangular plate with free edges," *Teor. Prikl. Mekh.*, **46**, 104–111 (2009).
5. R. Aghababaei and J. Reddy, "Nonlocal third-order shear deformation plate theory with application to bending and vibrations of plates," *J. Sound Vibr.*, **326**, No. 1, 227–286 (2009).
6. B. Akgoz and O. Civalek, "Nonlinear vibration analysis of laminated plates resting on nonlinear two-parameters elastic foundations," *Steel Compos. Struct.*, **11**, No. 5, 403–421 (2011).
7. A. V. Altukhov and M. V. Fomenko, "Elastic vibrations of sandwich plates with diaphragms at the edges," *Int. Appl. Mech.*, **50**, No, 2, 179–186 (2014).
8. R. Azarafza, "Fabrication, experimental modal testing, and a numerical analysis of composite sandwich structures with a grid-stiffened core," *Mech. of Comp. Mat.*, **54**, No. 4, 537–544 (2018).
9. R. C. Barta, L. F. Qian, and L. M. Chen, "Natural frequencies of thick square plates made of orthotropic, trigonal, monoclinic, hexagonal and triclinic materials," *J. Sound and Vibr.*, **270**, No. 4–5, 1074–1086 (2004).
10. A. Bessaim and et al., "A new third-order shear and normal deformation theory for the static and free vibration analisis of sandwich plates with functionally graded isotopic face sheets," *J. Sandwich Struct. Mater.*, **15**, No. 6, 671–703 (2013).
11. E. I. Bespalova, "Determining the natural frequencies an elastic parallelepiped by the advanced Kantorovich–Vlasov method," *Int. Appl. Mech.*, **47**, No. 4, 410–421 (2011).
12. E. I. Bespalova and G. P. Urusova, "Three-dimensional analysis of the lower frequencies of a cantilevered anisotropic parallelepiped," *Int. Appl. Mech.*, **50**, No. 4, 367–377 (2014).
13. V. Birman and L. W. Byrd, "Modeling and analysis of functionally graded materials and structures," *Appl. Mech. Rev.*, **60**, No. 5, 195–216 (2007).
14. E. Carrera and S. Brischetto, "A survey with numerical assessment of classical and refined theories for the analysis of sandwich plates," *Appl. Mech. Rev.*, **62**, No. 1, 1–17 (2009).
15. D. J. Gorman and R. Singhal, "Free vibration analysis of cantilever plates with step discontinuities in properties by the method of superposition," *J. Sound Vibr.*, **253**, No. 3, 631–652 (2002).
16. Ya. M. Grigorenko, A. S. Bergulev, and S. N. Yaremchenko, "Numerical solution of bending problems for rectangular plates," *Int. Appl. Mech.*, **49**, No. 1, 81–94 (2013).
17. Ya. M. Grigorenko and A. Ya. Grigorenko, "Static and dynamic problems for anisotropic inhomogeneous shells with variable parameters and their numerical solution (review)," *Int. Appl. Mech.*, **49,** No. 2, 123–193 (2013).
18. A. P. Gupta, "Vibration of rectangular orthotropic elliptic plates on quadratically varying thickness on elastic foundation," *Trans. ASME, J. Vibr. Acoust.*, **126**, No. 1, 132–140 (2004).
19. K. Güler, "Circular elastic plate resting on tensionless Pasternak foundation," *J. Eng. Mech.*, *ASCE*, **130**, No. 10, 1251–1254 (2004).
20. A. N. Guz and N. A. Shulga, "Dynamics of laminated and fibrous composites," *Appl. Mech. Rev.*, **45,** No. 2, 35–60 (1992).

21. A. Houmat, "Three-dimensional free vibration analysis of plates using the *h-p* version of the finite element method," *J. Sound Vibr.*, **290**, No. 3–5, 690–704 (2006).
22. T. V. Karnaukhova and E. V. Pyatetskaya, "Resonant vibrations of a clamped viscoelastic rectangular plate," *Int. Appl. Mech.*, **45**, No. 8, 904–917 (2009).
23. V. V. Levchenko, "Effect of boundary conditions on the natural frequencies and vibration modes of piezoelectric plates with radially cut electrodes," *Int. Appl. Mech.*, **51**, No. 2, 187–195 (2015).
24. K. M. Liew, K. C. Hung, and K. M. Lim, "A continuum three-dimensional vibration analysis of thick rectangular plates," *Int. J. Solids Struct.*, No. 30, 3357–3379 (1993).
25. L. Liu and K. Bhattacharya, "Wave propagation in a sandwich structure," *Int. J. Solids Struct.*, **46**, No. 17, 3290–3300 (2009).
26. A. V. Marchuk, "Determination of the natural frequencies of vibration of nonuniform slabs," *Int. Appl. Mech.*, **35**, No. 2, 152–158 (1999).
27. A. V. Marchuk, S. V. Gnedash, and D. O. Shandyba, "Free and forced vibrations of thick-walled laminated anisotropic cylindrical shells with account for energy dissipation at frequencies close to resonance ones," *Compos.: Mech. Comput. Appl.*, **8**, No. 3, 239–265 (2017).
28. A. V. Marchuk and A. V. Nishchota, "On the strain–stress state of locally loaded layered composite slabs," *Int. Appl. Mech.*, **54**, No. 3, 315–330 (2018).
29. A. V. Marchuk and V. G. Piskunov, "Statics, vibrations, and stability of composite panels with gently curved orthotropic layers. 1," *Statics and vibrations, Mech. Comp. Mater.*, **35**, No. 4, 285–292 (1999).
30. O. G. McGee and G. T. Giaimo, "Three-dimensional vibrations of cantilevered right triangular plates," *J. Sound Vibr.*, **159**, No. 2, 279–293 (1992).
31. H. Nagino, T. Mikami, and T. Mizusawa, "Three-dimensional free vibration analysis of isotropic rectangular plates using the b-spline ritz method," *J. Sound Vibr.*, **317**, No. 1–2, 329–353 (2008).
32. Y. Qu and G. Meng, "Three-dimensional elasticity solution for vibration analysis of functionally graded hollow and solid bodies of revolution. Part I: Theory," *Europ. J. Mech. A, Solids*, No. 44, 222–233 (2014).
33. M. S. Qatu, *Vibration of Laminated Shells and Plates*, Elsevier Academic Press, Amsterdam (2004).
34. M. Rao and Y. Desai, "Analytical solution for vibrations of laminated and sandwich plates using mixed theory," *Compos. Struct.*, **63**, No. 3, 373–330 (2004).
35. N. A. Shulga, "Mixed systems of equations in Kirchhoff's theory of the transverse vibrations of plates," *Int. Appl. Mech.*, **49**, No. 2, 194–202 (2013).
36. Yu. V. Skosarenko, "Free vibrations of ribbed cylindrical shell interacting with an elastic foundation," *Int. Appl. Mech.*, **50**, No. 5, 575–581 (2014).
37. R. P. Shimpi and H. G. Patel, "Free vibrations of plate using two variable refined plate theory," *J. Sound Vibr.*, No. 296, 979–999 (2006).
38. W. Soedel, *Vibrations of Shells and Plates*, Marcel Dekker, Inc., New York (2004).
39. N. G. Stephen, "The second spectrum of Timoshenko beam theory – further assessment," *J. Sound Vibr.*, **292**, No. 1–2, 372–389 (2006).
40. N. G. Stephen and S. Puchegger, "On the valid frequency range of Timoshenko beam theory," *J. Sound Vibr.*, **297**, No. 3–5, 1082–1087 (2006).
41. F. Tornabene, N. Fantuzzi, E. Viola, and J. N. Reddy, "Winkler–Pasternak foundation effect on the static and dynamic analyses of laminated doubly-curved and degenerate shells and panels," *Compos., Part B, Eng.*, **57**, No. 1, 269–296 (2014).
42. T. M. Tu and N. H. Quoc, "Finite element modeling for bending and vibration analysis of laminated and sandwich composite plates based on higher-order theory," *Comput. Mater. Sci.*, **49**, No. 4, 390–394 (2010).
43. L. Woodcock Roland, B. Bhat Rama, and G. Stiharu Ion, "Effect of ply orientation on the in-plane vibration of single-layer composite plates," *J. Sound Vibr.*, **312**, No. 1–2, 94–108 (2008).